Magnetic properties of type-II superconductors with reduced phase stiffness

F. Horváth and R. Hlubina
Department of Experimental Physics, Comenius University, Mlynská Dolina F2, 842 48 Bratislava, Slovakia
(Received 28 January 2010; published 15 April 2010)

Motivated by the phenomenology of underdoped cuprates, we study a modified Ginzburg-Landau theory which describes type-II superconductors with reduced phase stiffness. The theory is characterized by three length scales: the penetration depth, λ, the amplitude coherence length, ξ, and the phase coherence length, $\xi_\perp$. Within the modified theory, we solve the single-vortex problem and calculate both, the lower and the upper critical fields H_{c1} and H_{c2}. We also present an approximate calculation of the equilibrium magnetization curve $M=M(H)$. Our results explain the difference in scaling of λ^{-2} and H_{c1} with the doping level in underdoped cuprates. Further experimental tests of our theory are proposed.

DOI: 10.1103/PhysRevB.81.134517 PACS number(s): 74.20.De, 74.25.Op, 74.72.Kf

I. INTRODUCTION

Within the conventional Ginzburg-Landau (GL) theory, superconductors are described in terms of the macroscopic wave function $\psi(\mathbf{r})$ which represents the center-of-mass motion of the Cooper pairs.[1–3] Being a complex function, $\psi(\mathbf{r})$ can be written in terms of an amplitude field $f(\mathbf{r})$ and a phase field $\theta(\mathbf{r})$

$$\psi(\mathbf{r}) = \psi_\infty f(\mathbf{r}) e^{i\theta(\mathbf{r})}.$$

For future convenience, we have normalized the amplitude field $f(\mathbf{r})$ so that in a homogeneous piece of a superconductor in which $\psi(\mathbf{r})=\psi_\infty$, we have $f(\mathbf{r})=1$.

The macroscopic wave function $\psi(\mathbf{r})$, together with the distribution of the magnetic field which is described by the vector potential $\mathbf{A}(\mathbf{r})$, are determined by minimization of a free-energy functional $\delta F=\int d^3\mathbf{r}\,\delta\mathcal{F}[\psi(\mathbf{r}),\mathbf{A}(\mathbf{r})]$. In the vicinity of the transition temperature T_c, the conventional GL free-energy density $\delta\mathcal{F}(\mathbf{r})$ can be written in the amplitude-phase language as

$$\delta\mathcal{F} = \frac{1}{2\mu_0}(\nabla\times\mathbf{A})^2 + \delta\mathcal{F}_s,$$

$$\frac{\delta\mathcal{F}_s}{\mu_0 H_c^2} = -f^2 + \frac{1}{2}f^4 + \xi^2(\nabla f)^2 + \xi^2 f^2\left(\nabla\theta + \frac{2\pi}{\Phi_0}\mathbf{A}\right)^2, \quad (1)$$

where H_c is the thermodynamic critical field and ξ is the coherence length. Note that the penetration depth λ_0 is not an independent parameter since it is given by

$$\lambda_0 = \frac{\Phi_0}{2\pi\sqrt{2}\mu_0 H_c \xi}. \quad (2)$$

Instead of the independent variables H_c and ξ, we could have parametrized the theory by two length scales, ξ and λ_0.

The crucial point to observe in Eq. (1) is that the amplitude fluctuations are equally expensive in energy as the phase fluctuations, both being measured by the same coherence length ξ. The key idea of the present paper is to remove this constraint and to introduce two different coherence lengths: one for the amplitude, ξ, and one for the phase, $\xi_\perp$. In doing so, we are motivated by the physics of underdoped cuprates, where it is often assumed that amplitude fluctuations of the superconducting order parameter are much more expensive in energy than the phase fluctuations. A substantial part of researchers even views the pseudogap region as a superconductor with a well-developed order parameter but without phase coherence,[4–6] or as a somewhat related phase-disordered liquid of resonating valence bonds, which roughly may be thought of as Cooper pairs.[7,8] In our language, they assume that in the pseudogap region there exists a finite amplitude stiffness $H_c^2\xi^2$ and, at the same time, a vanishing phase stiffness $H_c^2\xi_\perp^2$.

Instead of Eq. (1) we therefore consider the following modified free-energy density:

$$\delta\mathcal{F} = \frac{1}{2\mu_0}(\nabla\times\mathbf{A})^2 + \delta\mathcal{F}_s,$$

$$\frac{\delta\mathcal{F}_s}{\mu_0 H_c^2} = -f^2 + \frac{1}{2}f^4 + \xi^2(\nabla f)^2 + \xi_\perp^2 f^2\left(\nabla\theta + \frac{2\pi}{\Phi_0}\mathbf{A}\right)^2. \quad (3)$$

We have in mind the application of this theory to underdoped cuprates in their superconducting state and we assume that $\xi_\perp$ is much smaller than ξ so that the phase fluctuations become cheap. Moreover, under approaching the phase transition, i.e., as $T\to T_c$, we expect that the dimensionless ratio

$$s = \xi_\perp/\xi$$

decreases and at the transition point ultimately $s=0$.

The free-energy density $\delta\mathcal{F}$ depends on three fields: the amplitude field $f(\mathbf{r})$, the phase field $\theta(\mathbf{r})$, and the vector potential $\mathbf{A}(\mathbf{r})$. Minimization with respect to these fields yields three modified GL equations

$$-\xi^2\Delta f + \xi_\perp^2\left(\nabla\theta + \frac{2\pi}{\phi_0}\mathbf{A}\right)^2 f + f^3 = f, \quad (4)$$

$$\nabla\cdot\mathbf{j} = 0, \quad (5)$$

$$\nabla\times\mathbf{B} = \mu_0\mathbf{j}, \quad (6)$$

where we have introduced a vector field $\mathbf{j}$ which is easily recognized as the supercurrent density

$$\mathbf{j} = -\frac{f^2}{\mu_0 \lambda^2}\left(\mathbf{A} + \frac{\hbar}{2e}\nabla\theta\right). \tag{7}$$

In the expression for $\mathbf{j}$, we have introduced the penetration depth

$$\lambda = \frac{\Phi_0}{2\pi\sqrt{2}\mu_0 H_c \xi_\perp} = \frac{\lambda_0}{s}. \tag{8}$$

Note that our modified GL theory can be parametrized by three length scales: λ, ξ, and $\xi_\perp$. Sometimes, especially when comparing with the conventional GL theory, it will also be convenient to use λ_0, ξ, and s as independent parameters.

The aim of this paper is to study the magnetic properties of type-II superconductors described by Eq. (3). In particular, in Sec. II we numerically solve the single-vortex problem and thereby we determine the lower critical field H_{c1}. We also calculate the equilibrium magnetization curve $M=M(H)$ at fields slightly higher than H_{c1}. In Sec. III we calculate the upper critical field H_{c2} and we present an approximate result for the full magnetization curve $M=M(H)$. In Sec. IV we summarize our results for the magnetization curve in the limit $s\to 0$. In Sec. V we compare our results to experimental data on the cuprates. We show that the experimentally observed difference in scaling of λ^{-2} and H_{c1} with the doping level in underdoped cuprates[9–11] can be simply understood within the modified GL scenario and we propose further experimental tests of our theory.

II. ISOLATED VORTEX AND THE LOWER CRITICAL FIELD

We shall study the single-vortex problem making use of the cylindrical coordinates $\mathbf{r}=(r,\varphi,z)$. We assume that the phase field $\theta(\mathbf{r})=-\varphi$ and $\mathbf{A}=(0,A,0)$. Furthermore, both the amplitude f and the vector potential A are supposed to be functions only of the radial coordinate r. Under these assumptions, the modified GL equations can be written as

$$-\xi^2\left(f'' + \frac{1}{r}f'\right) + \frac{\xi_\perp^2}{r^2}(1-\phi)^2 f + f^3 = f, \tag{9}$$

$$\phi'' - \frac{1}{r}\phi' + \frac{f^2}{\lambda^2}(1-\phi) = 0, \tag{10}$$

where the primes denote the derivatives with respect to r and instead of $A(r)$ we consider a dimensionless flux threading a ring with radius r

$$\phi(r) = \frac{\Phi(r)}{\Phi_0} = \frac{2\pi A(r) r}{\Phi_0}.$$

Note that the second modified GL equation Eq. (5) is satisfied automatically by our ansatz and therefore it is not written down.

The modified GL Eqs. (9) and (10) have to be solved subject to the boundary conditions $\phi(0)=0$, $\phi(\infty)=1$, $f(0)=0$, and $f(\infty)=1$. In the limit $r\to 0$ we can neglect both $\phi(r)$ and f^3 in Eq. (9). Looking for a power-law solution we find that $f(r)\propto r^s$, i.e., the amplitude function exhibits a nonanalytic behavior near the origin. Our numerical data are in perfect agreement with this scaling. Since $s\ll 1$, the region where f is substantially suppressed with respect to the bulk value $f=1$, i.e., the vortex core, is extremely narrow. Explicit examples of the functions $f(r)$ for a representative value of the GL parameter $\kappa=\lambda/\xi=100$ are shown in Fig. 1.

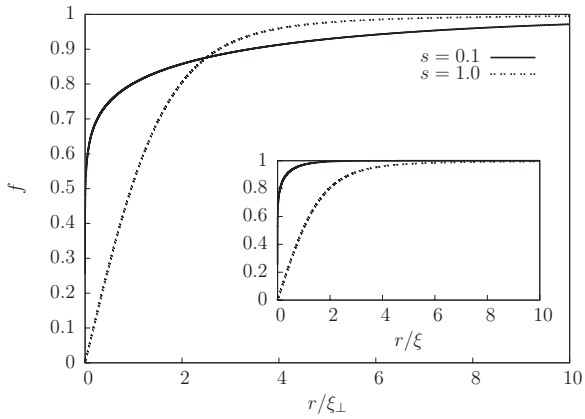

FIG. 1. The radial dependence of the amplitude function $f(r)$ in the vicinity of the vortex for $\kappa=100$ and two values of s.

A similar analysis shows that in the vicinity of the vortex core, i.e., for $r\to 0$, the magnetic field scales as $B(r)=B_0 - cr^{2s}$, where B_0 and c are constants. Numerical results shown in Fig. 2 are again in excellent agreement with this scaling. Note the sharp upturn of the magnetic field in the immediate vicinity of the vortex core. We have studied the dependence of the maximal field in the vortex core B_0 on s and κ in some detail. Figure 3 shows that, in a wide range of parameters, the following formula describes B_0 quite well:

$$B_0 = \frac{\Phi_0}{4\pi\lambda^2}\mathcal{B}_0; \quad \mathcal{B}_0 = \frac{1-3s^2/2}{s} + 2\ln\kappa. \tag{11}$$

In Figs. 2 and 3 we plot the dimensionless magnetic fields $\mathcal{B}(r)$ and $\mathcal{B}_0$, i.e., magnetic fields in units of $\Phi_0/(4\pi\lambda^2)$.

Finally, we have studied the lower critical field H_{c1} within our modified GL theory. To this end, we have to consider the

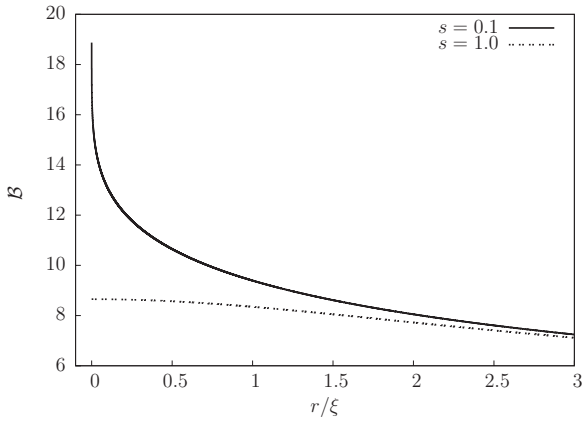

FIG. 2. The radial dependence of the dimensionless magnetic field $\mathcal{B}(r)$ in the vicinity of the vortex for $\kappa=100$ and two values of s.

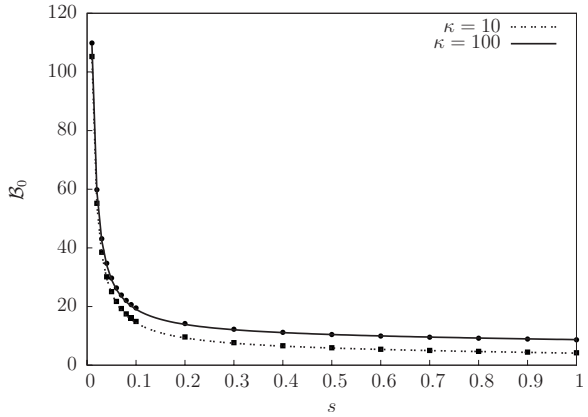

FIG. 3. The dimensionless maximal field $\mathcal{B}_0$ in an isolated vortex as a function of s. The lines are plots of the formula Eq. (11).

generalized Gibbs free-energy density in applied field H, $\delta\mathcal{F}-HB$, and compare the Gibbs free energy per unit length in the z direction in presence of a vortex, $\delta G_{\text{with}}=\int d^2\mathbf{r}\,\delta\mathcal{F}-H\Phi_0$, with its value in absence of a vortex, $\delta G_{\text{without}}=\int d^2\mathbf{r}(-\frac{1}{2}\mu_0 H_c^2)$. The lower critical field H_{c1} can be calculated by equating δG_{with} and $\delta G_{\text{without}}$

$$H_{c1}=\frac{1}{\Phi_0}\int d^2\mathbf{r}\left[\delta\mathcal{F}+\frac{1}{2}\mu_0 H_c^2\right], \tag{12}$$

$$=\frac{\pi}{\mu_0\Phi_0}\int_0^\infty drr[B^2+\mu_0^2 H_c^2(1-f^4)], \tag{13}$$

$$=\frac{2\pi\mu_0 H_c^2}{\Phi_0}\int_0^\infty drr(1-f^2). \tag{14}$$

The simplified Eqs. (13) and (14) can be derived by techniques which are well known in the standard GL theory.[1] We have calculated H_{c1} numerically using all three expressions, Eqs. (12)–(14), in order to check our numerics. As shown in Fig. 4, our results can be fit in a wide parameter region by the formula

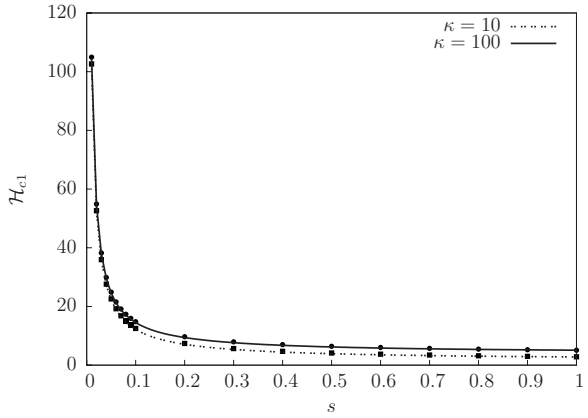

FIG. 4. The dimensionless lower critical field $\mathcal{H}_{c1}$ as a function of s. The lines are plots of the formula Eq. (15).

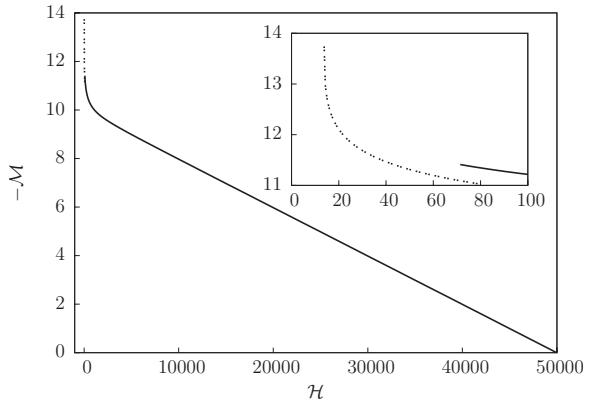

FIG. 5. Approximate magnetization curve $\mathcal{M}=\mathcal{M}(\mathcal{H})$ for $s=0.1$ and $\kappa=50$. The inset shows the detail of the magnetization curve in the vicinity of $\mathcal{H}_{c1}$. The low-field expansion described in Sec. II is shown by the dashed line.

$$H_{c1}=\frac{\Phi_0}{4\pi\mu_0\lambda^2}\mathcal{H}_{c1};\quad \mathcal{H}_{c1}=\frac{1}{s(1+s^2)}+\ln\kappa. \tag{15}$$

From now on, the magnetic field H and the magnetization M will be measured in units of $\Phi_0/(4\pi\mu_0\lambda^2)$. The dimensionless fields and magnetizations will be called $\mathcal{H}$ and $\mathcal{M}$, respectively.

Our next task is to determine the magnetization curve for fields slightly larger than H_{c1}. We assume that a triangular lattice is formed with a lattice constant $a\gg\xi$. Following standard analysis,[2] in this range of lattice constants we can approximate the Gibbs free energy as a sum of energies of free vortices and of the vortex-vortex interactions

$$\mathcal{G}(a)=\frac{2\Phi_0}{\sqrt{3}a^2}\left[H_{c1}-H+\frac{\Phi_0}{4\pi\mu_0\lambda^2}\sum_{\mathbf{r}}K_0\left(\frac{|\mathbf{r}|}{\lambda}\right)\right].$$

The summation over $\mathbf{r}$ in the formula for $\mathcal{G}$ is to be taken over all vectors connecting a given lattice point with the remaining points in the vortex lattice. Minimizing $\mathcal{G}(a)$ with respect to a, we find how $B=2\Phi_0/(a^2\sqrt{3})$ depends on the applied field H. Since the magnetization is given by $M=B/\mu_0-H$, we can finally determine the magnetization curve $M=M(H)$. Usually, one takes instead of the Bessel function $K_0(x)$ its large-distance asymptotics and restricts the sum to the six nearest neighbors of the given lattice point. We have taken the full Bessel function and we have studied the convergence of the resulting magnetization curve $M=M(H)$ with the number of shells around the given lattice point which are taken into account in the calculation of $\mathcal{G}(a)$. The result of this procedure is shown in the inset to Fig. 5.

III. UPPER CRITICAL FIELD AND THE MAGNETIZATION CURVE

The upper critical field H_{c2} can be determined by closely following Abrikosov's analysis within the standard GL theory. At H_{c2}, we expect that the magnetic field $\mathbf{B}$ is equal to the applied field $\mu_0\mathbf{H}$, therefore we can choose $\mathbf{A}=(0,\mu_0 Hx,0)$. Using the ansatz $\theta=ky$, Eq. (5) is trivially

solved. Moreover, since $f \to 0$, we can neglect the f^3 term in the GL Eq. (4); thus we have to solve the equation

$$-\xi^2 \Delta f + \xi_\perp^2 \left(k + \frac{2e\mu_0 H}{\hbar} x \right)^2 f = f.$$

One finds easily that this equation has solutions for the largest fields H, if the amplitude depends only on the coordinate x, $f=f(x)$. In this case we are dealing with an equation for a harmonic oscillator and it is easy to show that solutions exist only for applied fields smaller than H_{c2}, where

$$H_{c2} = \frac{\Phi_0}{2\pi\mu_0 \xi \xi_\perp}. \tag{16}$$

As a next step, we would like to solve the modified GL equations slightly below H_{c2}. This problem has been solved by Abrikosov by considering linear combinations of the solutions which are degenerate exactly at H_{c2}. We start the discussion by first showing that our modified GL theory is essentially nonlinear and, therefore, Abrikosov's approach cannot be easily modified to our case. In fact, let us first observe that addition of complex numbers $\psi=\psi_1+\psi_2$ can be easily performed if we express $\psi_{1,2}$ in terms of their real and imaginary parts; the real (imaginary) part of ψ is then simply the sum of the real (imaginary) parts of $\psi_{1,2}$. However, if we express $\psi_{1,2}$ in terms of their amplitudes $f_{1,2}$ and phases $\theta_{1,2}$, the amplitude and phase of ψ is given by complicated expressions of $f_{1,2}$ and $\theta_{1,2}$. This suggests that linear superpositions of an infinite number of solutions may be useful only in the language of real and imaginary parts. However, the gradient term in Eq. (3), when expressed in terms of the wave function $\psi(\mathbf{r})$, reads as

$$\psi_\infty^2 \left[\xi^2 (\nabla f)^2 + \xi_\perp^2 f^2 \left(\nabla\theta + \frac{2\pi}{\Phi_0}\mathbf{A} \right)^2 \right]$$
$$= \frac{\xi^2 + \xi_\perp^2}{2} |\mathbf{\Pi}\psi|^2 - \frac{\xi^2 - \xi_\perp^2}{4|\psi|^2} [(\psi^* \mathbf{\Pi}\psi)^2 + (\psi \mathbf{\Pi}^* \psi^*)^2], \tag{17}$$

where $\mathbf{\Pi} = -i\nabla + \frac{2\pi}{\Phi_0}\mathbf{A}$. Note that the first term on the right-hand side is quadratic in ψ, leading to a linear theory, but the second term, which is finite for $\xi_\perp \neq \xi$, leads to highly nonlinear gradient terms in the equations of motion.

Because of the above-mentioned difficulty, we have decided to construct an approximate vortex-lattice solution of the Wigner-Seitz type, which will be shown to be quite accurate both close to H_{c1} and to H_{c2}. Namely, we replace the elementary cell of the vortex lattice by a circular disk with radius d and inside the disk we look for solutions to the radially symmetric modified GL Eqs. (9) and (10). The boundary conditions in the center of the disk are $f(0)=0$ and $\phi(0)=0$ and at the circumference of the disk we require $f'(d)=0$ since the function $f(r)$ should be smooth in the periodic vortex lattice, and $\phi(d)=1$, since each vortex should carry exactly one flux quantum.

Let us first observe that our approximate solution reproduces the exact value Eq. (16) of the critical field H_{c2}. In fact, at the critical field $f \to 0$ and the solution to a linearized version of Eq. (10) reads as $\phi = \pi\mu_0 H_{c2} r^2/\Phi_0$. In order to satisfy the boundary condition $\phi(d)=1$, we therefore have to choose $d^2=\Phi_0/(\pi\mu_0 H_{c2})$. Introducing a dimensionless coordinate $\rho=r/L$ where $L^2=d^2/(2s)$, the modified GL Eq. (9) can be written as

$$f'' + \frac{1}{\rho} f' + \left[\frac{d^2}{2\xi\xi_\perp} - \left(\frac{\rho}{2} - \frac{s}{\rho} \right)^2 \right] f = 0, \tag{18}$$

where the primes denote derivatives with respect to ρ. For $d^2=2\xi\xi_\perp$, Eq. (18) has a solution $f \propto \rho^s e^{-\rho^2/4}$, which satisfies both $f(0)=0$ and $f'(d)=0$. Comparing the two expressions for d^2, $2\xi\xi_\perp=\Phi_0/(\pi\mu_0 H_{c2})$, we end up with an expression for H_{c2} identical with the exact solution Eq. (16). Magnetic fields $H>H_{c2}$ are not admissible because then we would have $d^2<2\xi\xi_\perp$. It is known that in that case Eq. (18) does not possess normalizable solutions since this is most likely because $f'(\rho)$ does not vanish, this strongly suggests that H_{c2} is the upper critical field of our approximate theory. Our numerical results are in perfect agreement with this observation.

Our next goal is to calculate the magnetization M as a function of the applied field H. To this end, we calculate the average free-energy density

$$\overline{\delta\mathcal{F}} = \frac{1}{\pi d^2} \int_S d^2\mathbf{r}\, \delta\mathcal{F},$$

where the integral is taken over the disk S with radius d. Note that $\overline{\delta\mathcal{F}}$ is a function of the average magnetic field $\bar{B} = \frac{\Phi_0}{\pi d^2}$. Let us perform the Legendre transformation to the Gibbs energy density $\overline{\delta\mathcal{G}}$ which is a function of H, $\overline{\delta\mathcal{G}}(H) = \overline{\delta\mathcal{F}}(\bar{B}) - H\bar{B}$. The optimal value of $\bar{B}$ for a fixed value of H can be found by minimizing $\overline{\delta\mathcal{G}}$ with respect to $\bar{B}$

$$\frac{\partial \overline{\delta\mathcal{G}}}{\partial \bar{B}} = 0, \quad H = \frac{\partial \overline{\delta\mathcal{F}}}{\partial \bar{B}}. \tag{19}$$

The latter equation, together with $\bar{B}=\mu_0 H + \mu_0 M$, allows us to calculate the magnetization curve $M=M(H)$.

Actual calculation of magnetization curves has been performed numerically. The average values $\overline{\delta\mathcal{F}}$ have been calculated using formulas analogous to both, Eqs. (12) and (13), enabling us to check the numerical accuracy. It is easy to see that the analog of Eq. (14) does not apply in the present case of finite d because for some of the per parts integrations needed to arrive at this formula the surface term does not vanish. Our numerical data shows that, in a wide range of parameters s and κ, the magnetization can be fitted in the vicinity of the upper critical field by the formula

$$M = -\frac{H_{c2} - H}{(2\kappa^2 - 1)\beta_A}, \tag{20}$$

which is of the same form as in the usual GL theory. As shown in Fig. 6, the parameter β_A depends only very weakly on s. It is worth pointing out that for $s=1$ we obtain $\beta_A \approx 1.147$, which is very close to the exact value for the triangular lattice[1] $\beta_A \approx 1.1596$. This suggests that our approximate results for the magnetization curve are very good in the vicinity of the upper critical field.

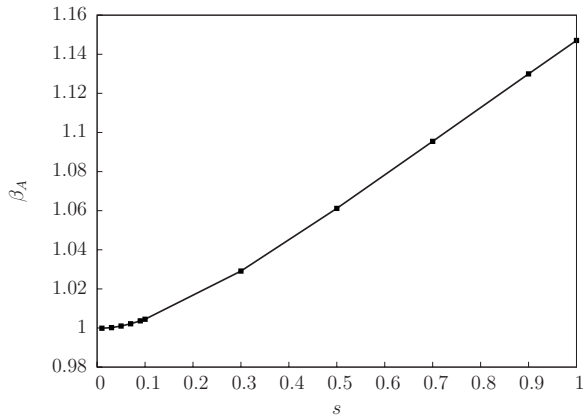

FIG. 6. Parameter β_A as a function of s for $\kappa=50$.

Let us note that the minimization procedure Eq. (19) correctly reproduces not only H_{c2} but also the lower critical field H_{c1}, which can be determined by comparing the minimized value $\overline{\delta\mathcal{G}}$ with $-\frac{1}{2}\mu_0 H_c^2$. Motivated by this observation, we have calculated the complete magnetization curve $M=M(H)$. The result is shown in Fig. 5. Comparison with the exact low-field expansion shows that our approximation is very good not only close to H_{c2} but also in the vicinity of the lower critical field. This leads us to assume that the full $M=M(H)$ curve is described with good accuracy.

Since there are three length scales in our problem, besides the characteristic magnetic fields H_{c1} and H_{c2} we have expected a feature of the magnetization curve at an intermediate field $H_{c1} \ll H^* \sim \Phi_0/(\mu_0\xi^2) \ll H_{c2}$. Surprisingly, Fig. 5 shows that there are no features in the $M=M(H)$ curve in the vicinity of the third characteristic magnetic field H^*.

IV. MAGNETIZATION CURVE FOR $s \to 0$

Let us summarize our results taking the triplet of parameters ξ, λ_0, and s as independent. In this language, the superconductor is characterized by three length scales: ξ, the amplitude coherence length, $\xi_\perp = s\xi$, the phase coherence length, and $\lambda = \lambda_0/s$, the weak-field penetration depth. The length scale λ determines the shielding properties of a weakly perturbed superconductor with $f \approx 1$, as is apparent from Eq. (7). Furthermore, in this language the thermodynamic critical field is independent of the parameter s, which measures the weakness of the phase stiffness

$$H_c = \frac{\Phi_0}{2\pi\sqrt{2}\mu_0\lambda_0\xi} = \frac{\Phi_0}{2\pi\sqrt{2}\mu_0\lambda\xi_\perp}.$$

It is instructive to write down the simplified expressions for the lower and upper critical fields in the limit $s \ll 1$

$$H_{c1} = \frac{\Phi_0 s}{4\pi\mu_0\lambda_0^2} \approx H_{c1}^0 \times s, \quad H_{c2} = \frac{\Phi_0}{2\pi\mu_0\xi^2 s} \approx H_{c2}^0 \times \frac{1}{s},$$

where the lower and upper critical fields of a usual GL superconductor with $s=1$ have been denoted H_{c1}^0 and H_{c2}^0, respectively.

This means that, under decreasing the parameter s from $s=1$, the thermodynamic field remains unchanged but the superconductor becomes more strongly type-II: the lower critical field decreases while the upper critical field increases. This might have been anticipated from the change in the GL parameter: initially it was $\kappa_0 = \lambda_0/\xi$ and it has increased to $\kappa = \lambda/\xi = \kappa_0/s$. All of this has to occur in such a way that the area under the magnetization curve does not change with s since from thermodynamic considerations we know that[2]

$$\int_0^{H_{c2}} (-M)dH = \frac{1}{2}H_c^2.$$

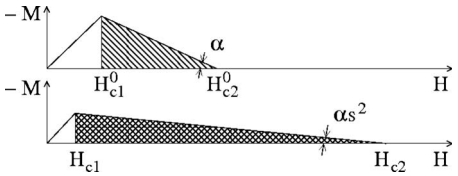

FIG. 7. Schematic of magnetization curves for a usual superconductor, $s=1$, and for a superconductor with reduced phase stiffness, $s=1/2$.

Our result Eq. (20) is in perfect qualitative agreement with this constraint: since $\kappa = \kappa_0/s$ and since β_A is roughly independent of s, the slope of the magnetization curve decreases by a factor s^2 with respect to the usual superconductor. This is exactly what is needed: the magnetization has to rise to an s-times smaller height on a s^{-1}-times larger distance, see Fig. 7.

V. COMPARISON TO EXPERIMENTAL DATA ON UNDERDOPED CUPRATES

Although the GL theory is strictly applicable only close to T_c, in what follows we will assume, in agreement with common practice, that it does describe, at least qualitatively, also the low-T physics. At low temperatures we expect that reducing the doping, x, toward the critical doping x_c for the appearance of superconductivity plays a similar role as increasing the temperature toward T_c: in both limits, s vanishes.

It is worth pointing out that in the underdoped cuprates, there exist two natural energy scales: the low-temperature energy gap Δ and the critical temperature T_c, which are vastly different and $\Delta \gg T_c$, unlike in a simple BCS superconductor. Therefore, as has been repeatedly pointed out,[12–14] one can introduce two natural coherence lengths: $\hbar v_F/\Delta$ and $\hbar v_F/T_c$. If we want to identify these two length scales with our length scales, then we have to require $\xi(0) \sim \hbar v_F/T_c$. We do get such an estimate from Eq. (2), if we take for the condensation energy $\mu_0 H_c^2(0) \sim N(0)T_c^2$ where $N(0)$ is the density of states at the Fermi level and if we estimate $\lambda_0(0)$ by the standard formula without any Fermi-liquid corrections. Furthermore, if we require $\xi_\perp(0) \sim \hbar v_F/\Delta$, then we get an estimate $s(0) \sim T_c/\Delta$. Note that this suggests that on approaching the critical doping, $\xi_\perp(0)$ stays more or less constant, whereas it is $\xi(0)$ which diverges, but in such a way that $H_c(0)\xi(0)$ stays constant as $T_c \to 0$.

The most straightforward argument against the applicability of the conventional GL theory to underdoped cuprates is as follows. Recent experiments on a set of high-quality un-

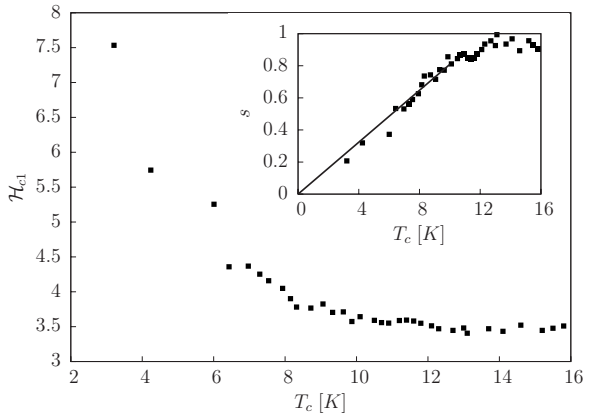

FIG. 8. Doping dependence of the dimensionless lower critical field $\mathcal{H}_{c1}$. The data points were determined making use of Eq. (15) from the experimental data for $\lambda=\lambda(T_c)$ in Ref. 10 and from the empirical formula for $H_{c1}=H_{c1}(T_c)$ proposed in Refs. 9.[15] The inset shows $s=s(T_c)$ determined from the data in the main panel using Eq. (15) and assuming $\ln\kappa=2.9$. The line is a linear fit to the data for $T_c\leq 10$ K.

derdoped $YBa_2Cu_3O_{7-x}$ samples have studied the dependence of the lower critical field[9] and of the weak-field penetration depth[10,11] on the doping level. From now on we will parameterize the doping level x by the corresponding transition temperature $T_c(x)$ and we assume that at critical doping $T_c(x_c)=0$. The dimensionless lower critical field $\mathcal{H}_{c1}$ extracted from the two data sets of Refs. 9 and 10 is shown in Fig. 8. According to Eq. (15), within the conventional GL theory with $s=1$, the dimensionless lower critical field $\mathcal{H}_{c1}$ should be constant, up to a weak logarithmic correction if κ depends on the doping level. The data in Fig. 8 is therefore clearly inconsistent with the conventional GL theory.

It is worth pointing out that the doping dependence of $\mathcal{H}_{c1}$ cannot be attributed to the fact that the first vortices enter into the defect positions and that, therefore, the value of H_{c1} depends on the amount of disorder in the sample. In fact, if this mechanism were operative, then $\mathcal{H}_{c1}$ should deviate downwards from the intrinsic value. The downward deviation should be strongest in the most disordered, i.e., the most underdoped sample, in contradiction to the experimentally observed upturn of $\mathcal{H}_{c1}$ in the extremely underdoped region.

In what follows, we will show that the results for the doping dependence of $\mathcal{H}_{c1}$ find a natural explanation within the modified GL theory. Our key assumption is that for underdoped samples we have the scalings

$$s(0)\propto T_c^{\alpha};\quad \xi(0)\propto T_c^{-\beta};\quad \lambda(0)\propto T_c^{-\gamma} \tag{21}$$

with exponents α,β,γ. This assumption is completely outside the realm of our classical theory and it should be considered as pure phenomenology. However, once this assumption is made, within the modified GL theory we can predict the scaling exponents of other observables; these predictions are summarized in Table I.

Let us first note that, according to Ref. 10, the weak-field penetration depth in the $YBa_2Cu_3O_{7-x}$ system scales differently with T_c in what we call extremely underdoped samples with $T_c\lesssim 12$ K where $\gamma=1$, and in moderately underdoped samples with $T_c\gtrsim 12$ K where $\gamma=0.5$. Around $T_c\sim 12$ K also the exponents α and β may change. Further evidence for this point of view is presented in the inset in Fig. 8 which shows that if we take $\ln\kappa\approx 2.9$, then samples with $T_c\lesssim 12$ K have $s<1$, whereas in samples with $T_c\gtrsim 12$ K we have $s\approx 1$. In other words, the value $T_c\sim 12$ K divides the samples with and without appreciable phase fluctuations.

In what follows we will analyze only the extremely underdoped region. The inset in Fig. 8 shows that the experimental data is not inconsistent with the exponent $\alpha\approx 1$ expected from $s(0)\sim T_c/\Delta$. As can be seen from Table I, the remaining exponent β can be found, e.g., from the condensation energy $\mu_0 H_c^2(0)/2$, which can, in principle, be determined from the specific-heat measurements. Unfortunately, such an analysis seems to have been performed only for moderately underdoped samples.[16] On the other hand, very careful measurements of the upper critical field $H_{c2}(0)$ (which has been called H_0) in underdoped samples of $La_{2-x}Sr_xCuO_4$ have been reported in Ref. 17. From their data we find $H_{c2}(0)\propto T_c^{0.7}$. Using the known value of α we would have to conclude that $\beta\approx 0.85$. However, since this value does not satisfy the bound $\beta\geq\alpha$ expected because $\xi_\perp$ should not vanish as $T_c\to 0$, we speculate that probably the extremely underdoped region has not been tested. In absence of additional information, we therefore assume that $\beta\approx 1$, as expected from $\xi(0)\sim\hbar v_F/T_c$.

In the last line of Table I we list the consequences of the experimental values $\alpha=\gamma=1$ and of the hypothesis $\beta\approx 1$. In particular, note that outside the superconducting dome the amplitude stiffness $H_c\xi$ is finite and the phase stiffness $H_c\xi_\perp$ vanishes, in agreement with the disordered superconductor picture of the pseudogap.

In the rest of this paper, let us discuss further experimental tests of the applicability of the modified GL theory to underdoped cuprates. According to Fig. 1, for $s<1$ the nor-

TABLE I. Predictions of the modified GL theory for the scaling exponents in the extremely underdoped region with $s\ll 1$. Exponents marked by * were calculated using $\beta\approx 1$ and the scaling relations.

	$s(0)$	$\xi^{-1}(0)$	$\lambda^{-1}(0)$	$\xi_\perp^{-1}(0)$	$\kappa(0)$	$H_{c1}(0)$	$H_{c2}(0)$	$\mu_0 H_c^2(0)/2$	$H_c(0)\xi(0)$	$H_c(0)\xi_\perp(0)$
Scaling				$1/(s\xi)$	λ/ξ	$1/(s\lambda^2)$	$1/(\xi^2 s)$	$1/(\lambda\xi s)^2$	$1/(\lambda s)$	$1/\lambda$
Exponent	α	β	γ	$\beta-\alpha$	$\beta-\gamma$	$2\gamma-\alpha$	$2\beta-\alpha$	$2(\beta+\gamma-\alpha)$	$\gamma-\alpha$	γ
Experiment	1[a]	≈ 1*	1[b]	≈ 0*	≈ 0*	1	≈ 1*	≈ 2*	0	1

[a]References 9 and 10.
[b]References 10 and 11.

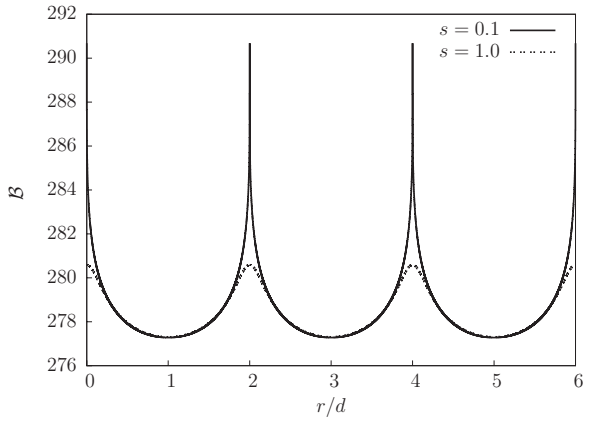

FIG. 9. Magnetic field profile along a line passing several vortex cores of a vortex lattice with $d=12\xi$ and $\kappa=100$ for $s=0.1$ (upper line) and $s=1$ (lower line).

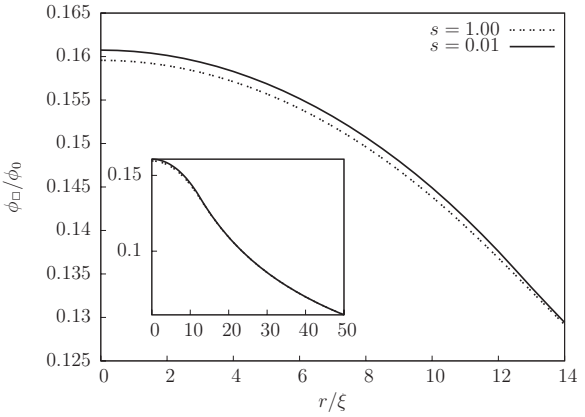

FIG. 10. Magnetic flux through a square loop $L\times L$ with $L/\lambda=0.25$ as a function of the position of the loop center, as the loop is moved along a line through the core of an isolated vortex with $\kappa=100$. The inset shows that, surprisingly, there is practically no difference between the $s=0.01$ and the $s=1.0$ data for $r/\xi=25$, i.e., when the loop passes the vortex center.

mal core is substantially suppressed compared with the conventional GL theory. Naively one would therefore expect that the local density of states in the vortex core is very different from the predictions of the weak-coupling BCS theory. Scanning tunneling spectroscopy does show such differences in the vortex cores of cuprate superconductors.[18] However, the modified GL theory cannot be directly compared to these experiments since the calculation of the density of states requires a fermionic model. Moreover, as shown by Berthod,[19] the core states are determined primarily by the phase field of the order parameter and not by its magnitude; therefore one should not seek a direct explanation of the anomalous local density of states in the modified GL theory. However, it is worth pointing out that some aspects of the vortex-core spectra have been captured by a microscopic model with an additional length scale[20] which is somewhat related to our modified GL theory.

We can further ask whether there is evidence for the existence of two different length scales in the scanning tunneling data. The spectra in overdoped samples seem to be governed by a single-length scale, see Figs. 46 and 49 in Ref. 18. Unfortunately, we are not aware of similar studies in underdoped cuprates.

Our theory makes a very specific prediction for the magnetic field profile in the vortices: for $s\ll 1$, there should exist sharp peaks in their centers, see Fig. 2 as well as Fig. 9, where the magnetic field profile along a line passing several vortex cores of a vortex lattice is shown. Such peaks might, in principle, be observable by local magnetic field probes such as scanning superconducting quantum interference device (SQUID) (Ref. 21) and Hall probe[22] microscopies. We have calculated the magnetic flux through a square loop $L\times L$ as a function of the position of the loop center, as the loop is moved along a line through the vortex core. We have taken $L=0.5$ μm, as appropriate for the state-of-art scanning Hall probe microscopes[22] which currently have a better spatial resolution than the scanning SQUID microscopes[21] with $L=8$ μm. We have also assumed that use is made of extremely underdoped samples with $T_c=3$ K which have a large penetration depth[10] $\lambda\approx 2$ μm, thus implying a favorable ratio $L/\lambda\approx 0.25$. However, Fig. 10 shows that even if the parameter s were as small as $s=0.01$, the experimental signal would be hardly distinguishable from the conventional case with $s=1$. This shows that the predictions of the modified GL theory for the magnetic field profile are unfortunately beyond the current resolution of the scanning SQUID and Hall probe microscopies.

It seems to be more promising to measure the magnetic field profile in an isolated vortex by means of magnetic-force microscopy. However, in this case one would have to minimize the backaction of the microscope on the vortex.[23] Another possibility would be to study the magnetic field distribution in the vortex lattice Fig. 9, either by small-angle neutron scattering,[24] or by the muon spin-rotation technique.[25] A more detailed analysis of the latter possibility is postponed to future work.

VI. CONCLUSIONS

In the first four sections of this paper, we have introduced and analyzed a modified GL theory with independent values of the amplitude and phase stiffness. The gradient terms in the free-energy density have a natural form in the amplitude-phase representation Eq. (3) but when written in terms of the real and imaginary parts of the GL wave function $\psi(\mathbf{r})$ in Eq. (17), they are seen to introduce additional nonlinearities. These nonlinearities lead to some unconventional properties of the vortices, such as the fractional power law of the order parameter $f(r)\propto r^s$ and the sharp peak of the magnetic field in the vortex center.

In Sec. V we have applied our results to experimental data on underdoped cuprates. The apparent inconsistency between the weak-field penetration depth and the lower critical field data, Fig. 8, can be naturally explained within the modified GL theory. In order to facilitate further tests of our theory, we have postulated power-law scalings, Eq. (21), of the three characteristic length scales of the modified GL theory with the doping level. Making use of these power laws, we have predicted the scaling of several observable quantities, such as

H_{c1}, H_{c2}, and the condensation energy. Together with the directly measurable weak-field penetration depth, we can thus obtain four experimental constraints on the three exponents α, β, γ. Our theory is therefore experimentally falsifiable. More detailed measurements of H_{c1}, H_{c2}, and the condensation energy on the extremely underdoped $YBa_2Cu_3O_{7-x}$ samples studied in Ref. 10 are necessary in order to confirm the preliminary results reported in Table I. Another possibility to test the modified GL picture is to study the magnetic field profile in an isolated vortex or in the vortex lattice.

ACKNOWLEDGMENTS

This work was supported by the Slovak Research and Development Agency under Grants No. APVV-51-003505, No. APVV-0432-07, and No. VVCE-0058-07, and by the Slovak Scientific Grant Agency under Grant No. 1/0096/08.

[1] A. Fetter and P. C. Hohenberg, in *Superconductivity*, edited by R. D. Parks (Marcel Dekker, New York, 1969), Vol. 2, p. 817.
[2] M. Tinkham, *Introduction to Superconductivity*, 2nd ed. (Dover, New York, 2004).
[3] K. H. Bennemann and J. B. Ketterson, *Superconductivity* (Springer, Berlin, 2008).
[4] V. J. Emery and S. A. Kivelson, Nature (London) **374**, 434 (1995).
[5] Y. Wang, L. Li, and N. P. Ong, Phys. Rev. B **73**, 024510 (2006).
[6] J. Orenstein, J. Corson, S. Oh, and J. N. Eckstein, Ann. Phys. **15**, 596 (2006).
[7] P. W. Anderson, P. A. Lee, M. Randeria, T. M. Rice, N. Trivedi, and F. C. Zhang, J. Phys.: Condens. Matter **16**, R755 (2004).
[8] P. A. Lee, N. Nagaosa, and X.-G. Wen, Rev. Mod. Phys. **78**, 17 (2006).
[9] R. Liang, D. A. Bonn, W. N. Hardy, and D. Broun, Phys. Rev. Lett. **94**, 117001 (2005).
[10] D. M. Broun, W. A. Huttema, P. J. Turner, S. Özcan, B. Morgan, R. Liang, W. N. Hardy, and D. A. Bonn, Phys. Rev. Lett. **99**, 237003 (2007).
[11] G. C. Kim, M. Cheon, S. S. Ahn, J. H. Jeong, and Y. C. Kim, EPL **81**, 27005 (2008).
[12] P. A. Lee and X.-G. Wen, Phys. Rev. Lett. **78**, 4111 (1997).
[13] L. B. Ioffe and A. J. Millis, Phys. Rev. B **66**, 094513 (2002).
[14] T. Senthil and P. A. Lee, Phys. Rev. B **79**, 245116 (2009).
[15] Further measurements are needed to fully confirm that the scaling $H_{c1}(0) \propto T_c^{1.64\pm0.04}$ found in Ref. 9 is valid also in the extremely underdoped region $T_c \lesssim 12$ K.
[16] J. W. Loram, J. Luo, J. R. Cooper, W. Y. Liang, and J. L. Tallon, J. Phys. Chem. Solids **62**, 59 (2001).
[17] L. Li, J. G. Checkelsky, S. Komiya, Y. Ando, and N. P. Ong, Nat. Phys. **3**, 311 (2007).
[18] Ø. Fischer, M. Kugler, I. Maggio-Aprile, C. Berthod, and C. Renner, Rev. Mod. Phys. **79**, 353 (2007).
[19] C. Berthod, Phys. Rev. B **71**, 134513 (2005).
[20] C. Berthod and B. Giovannini, Phys. Rev. Lett. **87**, 277002 (2001).
[21] J. C. Wynn, D. A. Bonn, B. W. Gardner, Y.-J. Lin, R. Liang, W. N. Hardy, J. R. Kirtley, and K. A. Moler, Phys. Rev. Lett. **87**, 197002 (2001).
[22] J. W. Guikema, H. Bluhm, D. A. Bonn, R. Liang, W. N. Hardy, and K. A. Moler, Phys. Rev. B **77**, 104515 (2008).
[23] L. Luan, O. M. Auslaender, D. A. Bonn, R. Liang, W. N. Hardy, and K. A. Moler, Phys. Rev. B **79**, 214530 (2009).
[24] For a recent application see, e.g., S. P. Brown, D. Charalambous, E. C. Jones, E. M. Forgan, P. G. Kealey, A. Erb, and J. Kohlbrecher, Phys. Rev. Lett. **92**, 067004 (2004).
[25] J. E. Sonier, J. H. Brewer, and R. F. Kiefl, Rev. Mod. Phys. **72**, 769 (2000).